Exactly solvable models of forced polymer loops.

Wenwen Huang,[1] Yen Ting Lin,[1] Daniela Frömberg,[1] Jaeoh Shin,[1] Frank Jülicher,[1] and Vasily Zaburdaev[1]

[1] *Max Planck Institute for the Physics of Complex Systems, Nöthnitzer Str. 38, D-01187 Dresden, Germany*

In this article, we present a one-dimensional model of pinned polymer loops in an external force field, which is motivated by the oscillatory motion of chromosomal loops during meiosis in fission yeast cells. This model unites several prominent concepts of statistical physics. We show that the steady state statistics of the forced polymer loop can be approximated by a combination of Fermi-Dirac and Brownian bridge statistics, while the exact solution is found by using the fermion integer partition theory. To solve for the dynamics of the forced polymer loop, we map it to a particle system of asymmetric simple exclusion process (ASEP) with reflecting boundary conditions. With the help of the generalized Bethe-Ansatz we analytically solve for its dynamics and obtain the longest relaxation time of the system. Finally, we show that this relaxation time as a function of applied force accurately describes the relaxation dynamics of the three-dimensional polymer loop obtained from numerical simulations and thus demonstrates the potential of the developed theory in biophysical applications.

I. INTRODUCTION

Simple models in polymer physics capture a certain set of generic polymer features [10, 11]. However, these features are often very robust and determine the physics of the experimentally observed systems. Rouse model representing a polymer as a chain of beads connected by harmonic springs [**?**] and its generalization to treat hydrodynamic interactions between the beads by Zimm [**?**] was successful in describing various aspects of polymer dynamics, relaxation and rheology []. Freely jointed chain model [] can be used to calculate the possible spatial configurations of the polymer. Thus even this simple model might be of relevance in the regimes when the free energy is dominated by the entropic part contribution [].

One good example is the success of the freely jointed chain model [10, 11] in understanding the dynamics and statistics of the DNA molecules: from *in vivo* mechanical properties of stretched DNA strands [1–3] to *in vitro* chromosomal territories [4–8], and hiC data [9].

Recently the freely jointed chain model was used to approach the problem of chromosome alignment by the drag forces during meiosis in fission yeast [3]. In yeast meiosis, homologous chromosomes are forming loops and are actively pulled through the viscous nucleoplasm in oscillatory fashion. On a half of the period of this oscillatory motion the pulling speed is nearly constant. The drag forces help to align chromosomes and allow for the process of recombination to happen. By assuming the steady state during this pull the nonequilibrium problem can be mapped on the equilibrium setting of a pinned polymer loop in an external field representing the drag force acting on the chromosomes. The statistics of the steady state configuration of the loop can be then obtained from a theory of random walks that are biased by the external force and have a requirement to return to origin to from the loop [3]. However, this analysis only provided predictions for the steady state, while leaving the dynamics of the process beyond its reach. Thus such important question as in what time and if the steady state can be reached on relevant time scales in the cell could be answered only with the help of numerical simulations.

In this paper, we show how the one-dimensional version of the pinned polymer loop model serves as a starting point of a chain of analogies that interlink several fields of statistical physics[12, 13] and provides the exact analytical solution to the dynamics of the loop. We first demonstrate that a synergy of the Brownian bridge theory and Fermi-Dirac statistics serves as an asymptotic approximation of the polymer loop statistics in the steady state. The exact solution can be found by solving the fermion number partition problem. We next show that the dynamics of the pinned polymer loop in an external force field can be mapped to an ASEP model [14–16] with reflecting boundary conditions. Via this link we can, on the one hand, immediately solve for the equilibrium statistics of the ASEP model and, on the other hand, investigate the dynamics of the polymer loop by means of the ASEP approach. Remarkably, the dynamics of the ASEP model can be solved exactly via the generalized Bethe-ansatz [17–19]. We find analytical predictions for the relaxation times of the system and use them to quantify the relaxation dynamics of the three-dimensional polymer loop as a function of the external force. We test all analytical results with extensive kinetic Monte-Carlo [20] and 3D Brownian dynamics simulations [21, 22].

Although our results focus on the loop geometry, we discuss possible generalizations to other constraints of the polymer. The interrelation of various prototypical statistical physics models, which we describe here, implies that methods developed for a particular problem can be ported to the other "relative" models as well. We thus think that the theoretical results presented here will be of interest to a broad and interdisciplinary scientific community working in the fields of polymer physics, number theory, and non-equilibrium statistical physics in general.

The manuscript is organized as follows. The next Section II is devoted to the polymer loop model and its steady state solution by a Brownian bridge theory and

relation to the integer number partition theory in one dimension. We then turn to the dynamics and the ASEP framework in Sec.III. In Sec.IV, we illustrate how the ASEP model can be utilized to study the polymer relaxation dynamics. The last Section is reserved for the discussion and conclusions.

II. STATISTICS OF THE ONE-DIMENSIONAL PINNED POLYMER LOOP

A polymer loop is a ubiquitous subject in polymer research pertinent to many important biological phenomena [3, 5, 7]. For example, fission yeast uses the viscous drag force to suppress fluctuations and align chromosomes for recombination by pulling on chromosomes arranged in a loop [3]. For a constant pulling speed this setting is equivalent to a pinned polymer loop in the uniform external force field [3], see Fig 1a. We start by setting up a one dimensional model of this process, see Fig. 1 for a sketch.

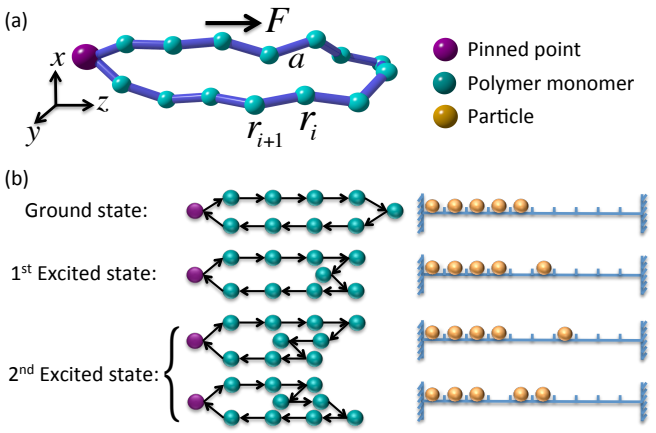

FIG. 1. Schematic figure for the model.

We consider a classical freely jointed chain model [11] consisting of L beads connected by L rods; the rod length corresponds to the Kuhn length a of the polymer. The position of the i^{th} bead is denoted by z_i, $i \in \{0, 1, \ldots, L\}$. The looping condition suggests $z_0 = z_L = 0$. A constant external force F acts on every bead (except of the pinned one) and points in the positive direction of the z-axis. We define the orientation of the i^{th} rod as $e_j := (z_j - z_{j-1})/a$ and therefore $z_i = a\sum_{j=1}^{i} e_j$ where $e_j = \pm 1$ and $i, j \in \{0, 1, \ldots, L\}$. In addition to regular forces, there are random forces acting on the chain. We will quantify their effect by an effective temperature T. We do not consider the volume exclusion effects and bending energy in this model.

Note that in the absence of force this model is equivalent to a trajectory of a one-dimensional unbiased random walk [26] consisting of L steps, where each step corresponds to a monomer (rod) in the chain. This random walk, however, has to start and end at the same point to fulfil the loop constraint. In mathematics, it is known as the Brownian bridge problem and can be solved to find the statistics of every bead position to be Gaussian with its variance depending on the number of the bead in the chain [3]. Therefore we can outline the strategy of solving the problem with a non-zero force: first find how the statistics of random walk steps changes in the presence of force and then enforce the Brownian bridge condition to form a loop.

To find the statistics of random walk steps (rod orientations) we write down the potential energy of the system:

$$E = -\sum_{i=1}^{L} F z_i = -Fa \sum_{i=1}^{L}\sum_{j=1}^{i} e_j, \tag{1}$$

We now map the polymer model to a particle system. Note that the state of rod orientation is binary, $e_j \in \{-1, +1\}$. We can map it to the state Z_j of a lattice site j, which is either occupied by a particle, $Z_j = 1$, when the rod points along the force or empty, $Z_j = 0$, if the rod points against the force, see Fig. 1b. The relation between Z_j and e_j is defined by a simple variable transformation $Z_j := (e_j + 1)/2$. The actual positions of polymer beads are obtained by the back transformation

$$z_i = a\sum_{j=1}^{i} e_j = a\left(2\sum_{j=1}^{i} Z_j - i\right). \tag{2}$$

By exchanging the order of the double summation in Eq. (1) and utilizing the loop condition $\sum_{j=1}^{L} e_j = 0$ we arrive at

$$E = \tilde{E} + \Delta E \sum_{j=1}^{L} j Z_j, \tag{3}$$

where $\tilde{E} = -L(L+1)\Delta E/4$ and $\Delta E = 2Fa$. The loop condition implies a hard constraint of the total number of the particles $\sum_{j=1}^{L} Z_j = L/2$ (there has to be equal number of steps along and against the force field to return to the origin).

A. Fermi-Dirac statistics of rod orientations

In the energy expression (3) one can immediately recognize the energy of a system of $L/2$ fermions distributed over L equidistant energy levels $\Delta E, \ldots, L\Delta E$, where Z_j can be interpreted as an occupation number. Clearly the lowest energy of the system corresponds to $Z_j = 1$ for $j < L/2$ and $Z_j = 0$ otherwise (fully stretched polymer loop), see Fig 1b. However, when the system is in contact with the thermal bath at temperature $T > 0$, it is possible to find other configurations. The equilibrium Gibbs measure defines the probability of the system to be in a certain configuration via the corresponding exponential Boltzmann factor. Interestingly, there are two possibilities to calculate those probabilities.

The fixed total number or particles $(L/2)$ corresponds to a picture of the *canonical ensemble* [12, 13]: the system does not exchange particles with its environment. However, the technical difficulty here is in finding all degenerate microscopic states corresponding to the given total energy of the system. Before venturing in this calculation we first look at the alternative, approximate solution.

An alternative approach is to relax the fixed-number constraint, and use the *grand canonical ensemble*, which allows exchange of particles with an external reservoir [12, 13], derive the probability distribution of the microscopic states to construct a random walk model, and then finally use the Brownian bridge condition to re-enforce the fixed-number constraint [3]. Under these assumptions, the statistics of the particles is now given by a solution to the standard fermionic problem. The probability distribution of Z_j is the *Fermi–Dirac* distribution [3, 12]:

$$\mathbb{P}\{Z_j = 1\} = \left\{1 + \exp\left[\frac{\Delta E\,(j-\mu)}{k_B T}\right]\right\}^{-1}, \tag{4a}$$

$$\mathbb{P}\{Z_j = 0\} = 1 - \mathbb{P}\{Z_j = 1\}, \tag{4b}$$

with a chemical potential $\mu = (L+1)/2$ obtained from the requirement that on average there are $L/2$ particles in the system. Noting the relation of Z_j and the orientation of j^{th} rod $e_j = (2Z_j - 1)$, the probabilities (4) can be used to compute the distribution of e_j. The Fermi–Dirac distribution shows that in the presence of the external force field the first half of the steps is biased in the direction of force, whereas the second half of steps has higher probability of pointing against the force field. We emphasize that only in the picture of the grand canonical ensemble, the probability distributions of each rod orientation are mutually independent. Given the probability distribution of the occupation number (rod orientation), their mean and variance can be easily calculated:

$$\mathbb{E}[Z_j] = \mathbb{P}\{Z_j = 1\}, \tag{5a}$$

$$\mathrm{var}[Z_j] = \mathbb{P}\{Z_j = 1\} \cdot \mathbb{P}\{Z_j = 0\} - \mathbb{E}[Z_j]^2. \tag{5b}$$

Now that we know the statistics of individual steps we can construct the corresponding random walk process. Let us look at its trajectory connecting beads k and l, $l > k$ and the corresponding propagator $\rho(z_l = z|z_k = 0)$. Remarkably, according to the Lindeberg-Feller central limit theorem [27, 28] this propagator is Gaussian with the mean and variance equal to the sum of mean and variance of all individual steps leading from bead k to l. We therefore found the statistics of random walks governing the polymer loop in the presence of the external force field. However, due to the grand canonical approach, such random walks would return to the origin only on average. While this random walk properly reproduces the mean position of every bead, but it is not able to predict the fluctuations of bead position. To work out the variance of the bead position we have to enforce the loop condition.

B. Imposing the Brownian bridge condition

The Brownian bridge condition is a straightforward formulation of the condition that a bead with an index i is a part of the loop of length L. The bead i belongs to the loop if two pieces of random walk trajectory of length i and $L-i$ respectively can meet at the position of the bead and belong to the same loop. Thus the probability density function of finding the bead in a given coordinate z is given by

$$\rho^L(z_i = z) = \frac{\rho(z_i = z|z_0 = 0)\,\rho(z_{L-i} = z|z_L = 0)}{\rho(z_L = 0|z_0 = 0)}, \tag{6}$$

where $\rho(z_k = z|z_j = 0)$ are the propagators of the corresponding random walk process. In case of the pinned polymer loop those propagators are Gaussian distributions with a mean and variance obtained as a sum of means and variances of all contributing individual steps of the random walk. Importantly, because each propagator entering the above Eq.(6) is Gaussian, the resulting $\rho^L(z_i = z)$ is Gaussian as well. Its variance is given by

$$\mathrm{var}\left[z_i^L\right] = \frac{\sum_{j=0}^{i}\mathrm{var}[Z_j]\sum_{j=L-i}^{L}\mathrm{var}[Z_j]}{\sum_{j=0}^{L}\mathrm{var}[Z_j]} \tag{7}$$

We can now use these results and compare with direct Monte-Carlo simulations of the one-dimensional pinned polymer loop in the external force field. In Fig. 2 we plot the mean (a) and variance (b) of every bead position for different strengths of the external force field. With increasing force the polymer becomes more stretched and fluctuations decrease. In the limit of zero force we recover the well known result of the standard Brownian bridge problem [27]. Although calculating the sums involved in the estimation of the mean and variance does not present any particular difficulty, for not too small temperatures the sums can be approximated by integrals and evaluated explicitly (see Appendix A for details).

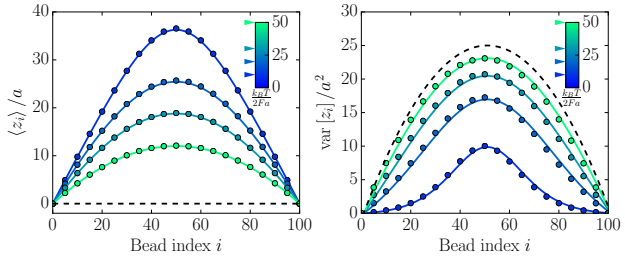

FIG. 2. Mean and variance of the 1D polymer loop.

In this section, we have shown that the combination of the Fermi–Dirac statistics following from the grand canonical treatment of the system together with the Brownian bridge condition for random walks provides an excellent approximation for the statistics of the pinned polymer loop. In the next section, for the sake of completeness we show how the same problem can be addressed exactly in the canonical ensemble picture.

C. Fermion integer number partition theory

Although the above approach accurately estimates the mean and variance of equilibrium position of every bead, it is an approximated theory. Exact analytic solution is possible in this particular model and helps to establish links to the number theory and theory of ASEP. First we change the basis of the fermionic system from its microscopic configurations $\{Z_1, Z_2, \ldots, Z_L\}$ to the total energy of the system. Clearly, the energy can only take values $E_0, E_0 + \Delta E, \ldots, E_0 + L^2\Delta E/4$ where E_0 is the ground state. In this picture, the probability space is a one-dimensional lattice with finite support. Without loss of generality, we set the constant energy $E_0 = 0$ and $\Delta E = 1$. The difficulty of this basis is to determine the degeneracy of the microscopic states which have the same energy $E \in \{0, 1, \ldots L^2/4\}$, referred to as the density of states in statistical mechanics [13] and condensed matter physics [29]. We denote the number of microscopic states with energy E to be $g(E)$; once $g(E)$ is known, the partition function of the system can be formally derived in the canonical ensemble picture

$$\mathcal{Z}(T) = \sum_{E=0}^{L^2/4} g(E) \exp\left(-\frac{E}{k_B T}\right), \tag{8}$$

and consequently the equilibrium properties of the system can be derived from it.

Interestingly the problem of finding $g(E)$ can be solved with the help of the closely related problem of integer partition in number theory [30]. The connection can be seen in the following way. Consider the system with the energy $E = \sum_{n=1}^{L/2} E_n$, where E_n is the energy of the n^{th} particle. Then $g(E)$ is the number of possible ways to partition integer E into the summation of $L/2$ integers with the constraint $0 \leq E_1 \leq E_2 \cdots \leq E_{L/2} \leq L/2$. A very intuitive way to visualize such microscopic configurations is to use the Young diagram [30]. From the number theory [30] we can find the generating function of $g(E)$ (see Appendix X), which turns out to be the Gaussian binomial coefficient:

$$\Phi(q) := \sum_{E=0}^{L^2/4} g(E) q^E = \begin{pmatrix} L \\ L/2 \end{pmatrix}_q \tag{9}$$

By comparing Eqs.(8) and (9) we can find an explicit and exact formula for the partition function of the polymer loop problem:

$$\mathcal{Z}(T) = \Phi\left(\exp\left(-\frac{\Delta E}{k_B T}\right)\right) \tag{10}$$

By knowing the exact partition function we can calculate the occupation probability of each site, see Appendix A. For large L the exact result is almost indistinguishable from our approximate theory based on Brownian bridges approach. However, for sufficiently small L the difference becomes more apparent (see Fig. 7 in Appendix A). Thus we have demonstrated that the polymer loop model can be related to and solved exactly in terms of the integer number partitioning problem. This, however, is not the last analogy we are going to utilize in this paper.

Here we have to note the connection of the considered problem to the ASEP setup on an interval with reflecting boundaries [14, 16] , where an analogous partition function was calculated [31]. This demonstrates the equivalence of our model of pinned polymer loop to the ASEP system with reflecting boundaries with exactly one half of the lattice sites occupied by the particles. In the next sections we further exploit this analogy to study the dynamics of the polymer loop model.

III. MAPPING TO ASEP

Above we considered a one-dimensional lattice with L lattice sites filled by $L/2$ particles. So far we were concerned only with the equilibrium properties of the system. However, by noticing the analogy to the ASEP model we can step beyond equilibrium considerations and study the dynamics of our system. To establish the link of the polymer loop model and the ASEP system we need to understand the relation between polymer dynamics and hopping rules of the ASEP. A particle occupying a lattice site corresponds to a monomer of the polymer loop pointing along the direction of force. Hopping of a particle on a lattice corresponds to the flipping of two monomers connecting to the same bead and having the opposite orientations with respect to the force field (see illustration in Fig. 3). During this flip, the bead has to travel a distance of $\pm 2a$. Indeed, just like in the exclusion process, the flip can occur only if there is a "free" lattice site. The asymmetry of the flipping results from the force acting on the beads: if, as a result of the flip, the bead moves along the force, it will be energetically more favorable than flipping the bead against the force. We can now formalize such dynamics by using the language of the ASEP model [14, 16]. We denote the rate of

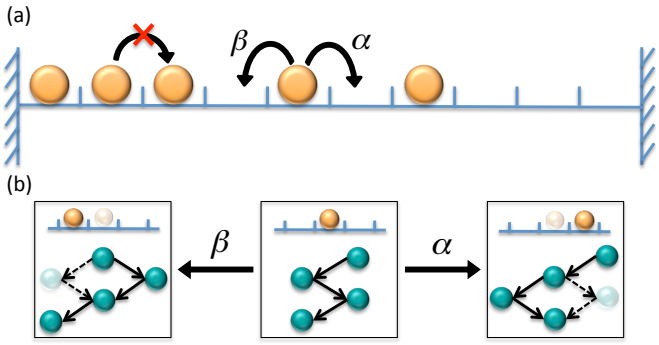

FIG. 3. Illustration of dynamics maps to ASEP.

particle hopping to the right and to the left with α and β respectively. For reflecting ASEP, the detailed balance

relation holds, so we have

$$\alpha P_l = \beta P_{l+1} \tag{11}$$

where P_l is the probability of a particle to occupy l^{th} site. The ratio of rates (and thus of the neighboring occupation probabilities) is proportional to the Boltzmann factor with the energy difference between the two states:

$$\alpha/\beta = P_{l+1}/P_l = \exp\left(-\Delta E/k_B T\right), \tag{12}$$

where $\Delta E = 2Fa$. The total hopping rate of a particle is determined by the effective temperature of the system:

$$\alpha + \beta = r_{\text{total}} \tag{13}$$

Hopping of a particle to the neighboring lattice site corresponds to flipping of two monomers and the displacement of the bead by a distance of $2a$. In the force-free case this flipping happens due to thermal fluctuations. Note that in the strictly one-dimensional setting, the monomers can not continuously turn, there are just initial and final states along or against the field. Therefore, for now we only provide an estimate of the time scale required for making a flip, a time for a bead to freely diffuse a distance $2a$

$$r_{\text{total}}^{-1} = \tau_0 = \frac{(2a)^2}{2D} = \frac{2\gamma a^2}{k_B T}. \tag{14}$$

where we used the diffusion constant of the bead given by Einstein relation $D = k_B T/\gamma$, where γ is the friction coefficient. Importantly, later we will be able to determine the proper calibration of this hopping rate by benchmarking our results with the Rouse theory (see below). Finally, from Eqs.(12,13) we obtain for the left and right hopping rates:

$$\alpha = \frac{r_{\text{total}} \exp\left(-2Fa/k_B T\right)}{1 + \exp\left(-2Fa/k_B T\right)} \tag{15a}$$

$$\beta = \frac{r_{\text{total}}}{1 + \exp\left(-2Fa/k_B T\right)} \tag{15b}$$

Next we need to specify the boundary conditions and if there any additional constraints on the number of particles. The pinned polymer loop corresponds to exactly $L/2$ particles hopping on L lattice sites with reflecting boundary conditions. The mapping can be generalized to other cases, for example, an un-pinned polymer loop corresponds to $L/2$ particles on L lattice sites with periodic boundaries, free polymer chain corresponds to an open lattice of length L filled by arbitrary (but not larger than L) number of particles.

ASEP is one of the fundamental models of non-equilibrium statistical physics with a wealth of important analytical results, see [14] for a review. However, not so many works are dealing with the particular case of reflective boundary conditions. One important contribution is due to Sandow and Schütz [31] where the partition function identical to Eq.(10) was derived. Here our main motivation is to get an insight on the dynamics of the system.

IV. EXACT SOLUTION OF ASEP DYNAMICS

We show that the exact analytical solution of the ASEP model with reflecting boundaries can be obtained by using the Bethe-ansatz [18, 19, 32]. To demonstrate the logic of derivation we first consider the simplest case of 2 particles on L-size lattice and then generalize it to arbitrary $N \leq L-1$.

A. Two particles

Let us denote $P(x_1, x_2; t)$ the time dependent probability of finding the first and the second particle at coordinates (x_1, x_2) respectively, where x_1, x_2 are integers. One can write down the master equation and boundary conditions which define the dynamics of the system, see appendix B. To solve for the dynamics, we first use the standard variable separation ansatz $P(x_1, x_2; t) = \sum_k \Psi_k(x_1, x_2) e^{\Lambda_k t}$. Now the task is to find Ψ_k and the corresponding eigenvalues Λ_k. The main idea of the generalized Bethe-ansatz is to use the general form of single-particle eigenfunctions as building blocks to construct Ψ_k (in contrast to plane waves in the standard Bethe-ansatz previously employed in the ASEP model with periodic boundaries [14, 32]). The ansatz we use here can be written as follows:

$$\Psi(x_1, x_2) = \psi_1(x_1)\psi_2(x_2) + \tilde{\psi}_2(x_1)\tilde{\psi}_1(x_2) \tag{16}$$

where $\psi_n, \tilde{\psi}_n, n = 1, 2$ are functions drawn from the following general form of the single-particle eigenfunctions:

$$\psi_s(x) = A\left(\tfrac{\alpha}{\beta}\right)^x \tag{17a}$$

$$\psi_{ns}(x) = \left(\tfrac{\alpha}{\beta}\right)^{\frac{x}{2}} \left(A_+ e^{ipx} + A_- e^{-ipx}\right) \tag{17b}$$

Here, A, A_+, A_- are amplitudes that will be fixed by the boundary conditions and normalization, p is the wave vector of the excited eigenmodes (in the case of a single particle $p = \frac{k\pi}{L}$, $k = 1, 2, ..., L-1$).

Following the single-particle terminology we will distinguish two classes of eigenfunctions: $\psi_s(x)$ given by Eq. (17a) to be referred to as stationary and $\psi_{ns}(x)$, Eq.(17b) non-stationary eigenfucntions. Now $\psi_n(x)$ with $n = 1, 2$ can be chosen from either class. Functions ψ_n and $\tilde{\psi}_n$ with and without tilde with the same subscript belong to the same class and have the same wave vector (in the non-stationary case) but may differ by the amplitudes.

There are three types of $\Psi(x_1, x_2)$ depending on the combination of $\psi_n(x)$ entering its definition Eq.(16): both stationary, both non-stationary, and the mixed type with one stationary and the other one non-stationary. The first case leads to the stationary mode of the two particles system with eigenvalue $\Lambda_0 = 0$ and $\Psi_0(x_1, x_2) = A\left(\frac{\alpha}{\beta}\right)^{x_1+x_2}$. A is a constant that can be fixed by normalization (for details see Appendix A for the general case of N particles).

The second type (both $\psi_n(x)$ are non-stationary) of $\Psi(x_1, x_2)$ when substituted in the boundary and exclusion conditions leads to the following system of Bethe equations [14] (see Appendix B for details):

$$e^{i2p_1L} = \frac{a(p_1,p_2)}{a(p_2,p_1)}\frac{a(p_2,-p_1)}{a(-p_1,p_2)} \tag{18a}$$

$$e^{i2p_2L} = \frac{a(p_2,p_1)}{a(p_1,p_2)}\frac{a(p_1,-p_2)}{a(-p_2,p_1)} \tag{18b}$$

where $a(p,p') = \sqrt{\alpha\beta}e^{i(p+p')} - (\alpha+\beta)e^{ip} + \sqrt{\alpha\beta}$. The corresponding eigenvalues can be calculated by $\Lambda = \sum_{n=1}^{2} -(\alpha+\beta) + 2\sqrt{\alpha\beta}\cos(p_n)$. Notice that by solving Eq. (18) we can get multiple pairs of roots because it is a set of nonlinear equations. So the number of eigenvalues we obtained from Eq. (18) is more than one.

The third type of $\Psi(x_1, x_2)$ (mixed) can be solved similarly to the second type. Interestingly, the resulting Bethe equation is very simple (we assumed that $\psi_1(x)$ is stationary):

$$e^{i2p_2L} = 1 \tag{19}$$

by solving which we get $p_2 = \frac{k\pi}{L}$ and the corresponding eigenvalues $\Lambda_k = -(\alpha+\beta) + 2\sqrt{\alpha\beta}\cos(p_2)$. These eigenvalues are exactly the same as for the single particle hopping on a lattice of size L with reflecting boundaries.

Thus we have shown how to employ the generalized Bethe-ansatz on the example of two particles. As the outcome we get three types of eigenstates: stationary, non-stationary with Bethe equations, and the mixed state leading to one-particle solution. We now show how to generalize this result to arbitrary N and discuss the general properties of the solution.

B. Generalization to N particles

The Bethe-ansatz for the N particle solution can be written as

$$\Psi(x_1, x_2, \cdots, x_N) = \sum_{\sigma\in\mathcal{S}_N}\prod_{n=1}^{N}\psi_n^{\sigma}(x_{\sigma(n)}) \tag{20}$$

where $\mathcal{S}_N$ is the group of permutations of N elements and ψ_n^{σ} is the n^{th} class of eigenfunction drawn from Eq. (17), either stationary or non-stationary. The subscript n means all functions in the n^{th} class share the same p_n, the superscript σ means the amplitude coefficients A_n^{σ} or $A_{n\pm}^{\sigma}$ are not the same for different permutations.

The stationary solution can be obtained by constructing Ψ only from stationary ψ_s, after normalization (see appendix A), we get:

$$P^e(x_1, x_2, \cdots, x_N) = q^{-\frac{N(N+1)}{2}}\binom{L}{N}_q^{-1}\prod_{j=1}^{N}q^{x_j} \tag{21}$$

here $q := \frac{\alpha}{\beta}$. The prefactor here is identical to the partition function from Sec.II C and the results of Ref.[31] where a method based on $U_q(SU(2))$ quantum group was utilized.

If all building blocks of Ψ are non-stationary, we arrive at the following Bethe equations:

$$e^{i2p_nL} = \prod_{m\neq n}^{N}\frac{a(p_n,p_m)}{a(p_m,p_n)}\frac{a(p_m,-p_n)}{a(-p_n,p_m)} \tag{22}$$

We can resolve them for p_n and find the corresponding eigenvalues $\Lambda = \sum_{n=1}^{N} -(\alpha+\beta) + 2\sqrt{\alpha\beta}\cos(p_n)$.

Finally let us consider the mixed case with N_s stationary building blocks in Ψ and $N - N_s$ non-stationary, where $0 < N_s < N$. One can show that the resulting Bethe equations are identical to the case of $N - N_s$ particles system when all building blocks are non-stationary. Moreover, the corresponding eigenvalues are $\Lambda = \sum_{n=1}^{N-N_s} -(\alpha+\beta) + 2\sqrt{\alpha\beta}\cos(p_n)$. Therefore we can conclude that the set of eigenvalues of N particle system always contains the set of eigenvalues of $N - N_s$ system given that $N < L/2$ (for $N > L/2$ we can instead look at vacancies and apply similar considerations). This is a generalization of the result of the two-particle system.

The central technical difficulty is to solve the Bethe equations to get the wave vectors and the corresponding set of the eigenvalues. It is a non-trivial task to show that the eigenstates obtained through the Bethe-ansatz approach indeed form a complete set, see for example [33]. We, so far, used the numerical solution of Bethe equations and compared thus obtained results for eigenvalues with the direct digitalization of the transition matrix in the master equation, see Fig. 4. In the figure we also show that the eigenvalues of the system with a smaller number of particles are always contained in the case of the system with larger N. Importantly, the subset of eigenvalues corresponding to the single particle solution can always be calculated explicitly:

$$\Lambda_k = -(\alpha+\beta) + 2\sqrt{\alpha\beta}\cos(\frac{k\pi}{L}); k = 1, 2, \ldots, L-1 \tag{23}$$

Numerical evidences shows that the single particle solution provides the largest non-zero eigenvalue ($k = 1$) which does not depend on the particles number N, thus giving us a direct estimate of the longest relaxation time in the system.

$$\tau = -\frac{1}{\Lambda_1} = \frac{1}{\alpha+\beta-2\sqrt{\alpha\beta}\cos(\frac{\pi}{L})} \tag{24}$$

Notice that an estimate of the relaxation time was also obtained in [31], and is different from our exact result Eq. (24) only by a factor $\sqrt{\alpha\beta}$.

C. Longest relaxation time

We can now consider an important limiting case of the general expression above, when L is large

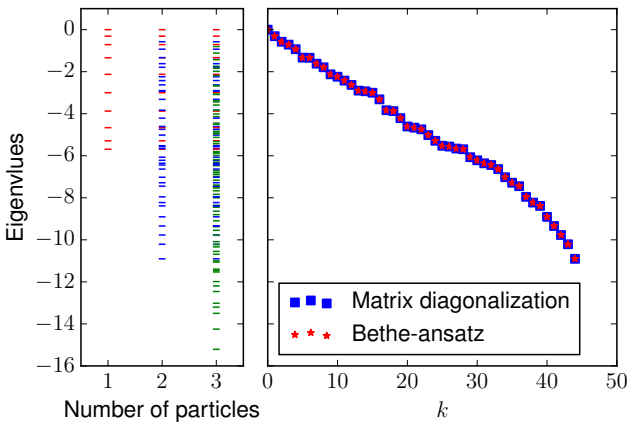

FIG. 4. eigenvalue obtained from directly diagonalizing the transition matrix and comparison with the results from Bethe-ansatz.

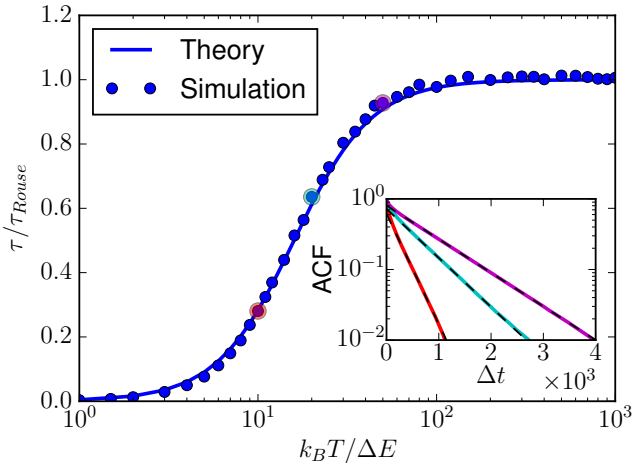

FIG. 5. relaxation time of ASEP for different force setting.

we can expand the cosine term and get $\tau = 1/\left((\sqrt{\alpha}-\sqrt{\beta})^2+\sqrt{\alpha\beta}\pi^2/L^2\right) \approx 1/(\sqrt{\alpha}-\sqrt{\beta})^2$. In the case of zero force $\alpha=\beta$, we arrive at

$$\tau = \frac{L^2}{\sqrt{\alpha\beta}\pi^2} = \frac{4L^2\gamma a^2}{k_BT\pi^2} \tag{25}$$

It is instructive at this point to recall the Rouse relaxation time of the classical bead-spring model, where a polymer is modeled as a chain of beads connected by ideal springs. The standard model [11] can be modified to explicitly accommodate the constraint of the pinned loop but retrieves the same standard Rouse time as for unconstrained chain. Interestingly the classical Rouse time is 4 times smaller. We can match the Rouse time in our bead-rod model if we make the following rescaling: $a \to a/2$. It is easy to understand as the rigid rod constrain in a way dictates two discrete extreme positions for the bead with a fixed separation, whereas in the Rouse model beads are allowed to move in one-dimensional space without any constraints in a continuous fashion. This rescaling will become even more intuitive in the following section.

To further test analytical predictions of this section we numerically investigated the process of relaxation in the one-dimensional pinned polymer loop by kinetic Monte-Carlo simulations. To quantify the relaxation times we looked at the time correlation function of the diameter of the polymer defined by $r_d = r_{L/2} - r_0$. For large times it shows an exponential decay, see inset in Fig.5. This allows us to determine the characteristic time of decaying correlations and associate it with the relaxation time of the loop. We see that the relaxation times plotted as a function of the external force match perfectly the analytical prediction given by the Bethe-ansatz solution, Eq.(24), see Fig 5.

Thus, starting from the biological problem of chromosome alignment we could unfold a very rich sequence of analogies and obtained the whole set of analytical results relevant for both polymer and non-equilibrium particle systems. To make the loop complete, now in the sense of paper structure, we would like to demonstrate how the above analytical results can be put to work in a more applied setting.

V. RELAXATION DYNAMICS OF A 3D POLYMER LOOP

Previously we argued that the stationary solution for the pinned polymer loop could be used to quantify the chromosome separation during meiosis in fission yeast [3]. However a very reasonable question is if the stationary state could be achieved on biologically relevant time scales. To answer this question we suggest to look at the relaxation dynamics of the pinned polymer loop as a function of parameters of the problem and in particular the applied external force. We performed extensive three-dimensional Brownian dynamics simulations of the relaxation process of the 3D polymer loop. By calculating the autocorrelation function of z component of diameter vector, we could extract the longest relaxation time of the polymer loop and plot it as a function of the applied force (see Fig.X). The relaxation times show the behavior very similar to our analytical prediction for the one-dimensional problem. We hypothesized that the functional form of Eq.(24) could be used to describe the results of the 3D simulations. Importantly, we know that the relaxation time in the limit of $F \to 0$ can be calculated from the Rouse-theory analytically. The result is identical to the 1D regime with an additional prefactor of 1/3 which arises due to the difference between 1D and 3D settings. We now can use this prefactor in the analytical formula Eq. (24) and a rescaled rod length $a \to a/2$ and plot it together with simulation results. Analytical (rescaled on the basis of the Rouse-theory) prediction matches the simulations very accurately. Note that there was no fitting involved when comparing theory and numerical data. Certainly the achieved agree-

ment of theory and data is a somewhat semi-empirical result, as we did not provide any three-dimensional theory except for the Rouse limit $F \to 0$. Nevertheless the one-dimensional model allows us to understand exactly the mechanisms responsible for the relaxation process in the system. It also makes it plausible to suggest that our results can be rigorously extended to higher dimensions. Here we should also comment that the one-dimensional bead rod system matches the 3D result after rescaling the rod length by a factor of 2. This is a natural result, as in 3D, the orientation of the rod changes continuously between two extreme values of pointing against or along the field, which are the only possibilities of the 1D model. Therefore rescaling a by a factor of 2 makes our model consistent with 1D Rouse model and with 3D polymer dynamics.

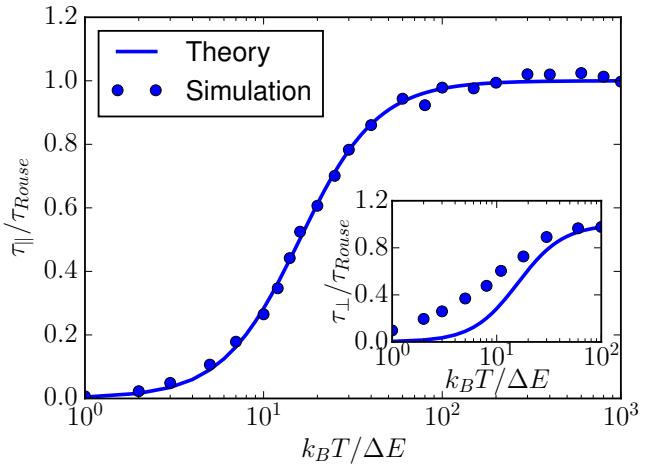

FIG. 6. relaxation time of 3D pinned polymer.

VI. CONCLUSIONS

A linear polymer chain with one end free and the other end pulled by an external force was studied both theoretically and experimentally. Pincus proposed a theory [34], which consider the pulled polymer as a sequence of independent "blobs". Brochard-Wyart further developed the "trumpet" and the "stem-flower" pictures of pulled polymer chain [35] in steady state. She also studied the stretch-coil relaxation of the pinned polymer chain. The retraction rate $L_0 - L \sim t^{1/2}$ was discovered. And the Rouse scaling $\tau \sim L^2$ for the recovery time was obtained. Using optical tweezer, Perkins et al. measured the stretch-coil relaxation a tethered DNA molecule with different lengths. The relaxation time, which is extracted from the decay of visual length, was found scaled as $\tau \sim L^{1.66}$ [36]. This result highlight the importance of hydrodynamic interaction in the real case. In our model, we measure the longest relaxation time from the autocorrelation function of the middle bead position. The Rouse scaling was recovered in the case of on external force. The retraction of the free end is linear with time initially and followed by a long exponential decay. So the $t^{1/2}$ scaling of retraction rate was not observed due to the missing of hydrodynamic interaction. Nevertheless, we track our model analytically and stress the important role of hydrodynamic interaction from the other side.

We demonstrated that the problem of the pinned 1D polymer loop in the external force field can be mapped to a system of particles hopping on lattice sites (ASEP). While the polymer problem can be asymptotically solved via the Brownian bridge formalism, in the ASEP formulation it has an exact solution. ASEP advances our understanding of the system to the dynamic regime. The key technique for the ASEP model solution is the generalized Bethe-ansatz, adding up to the Fermi-Dirac statistic as yet another unexpected appearance of quantum-mechanics tools in an original biophysical problem. Finally we could use those results to explain the force dependence of the relaxation times observed in 3D Brownian dynamics simulations.

In addition to the network of relations between different models and approaches we would like to mention yet another connection arising from the ASEP model. It is well known that ASEP models are often used as discrete counterparts of the single file diffusion process [37, 38]. In single file diffusion, particles are considered to be confined to a narrow one-dimensional channel which does not allow the particles to overcome each other. As the name implies, individual particles move by normal diffusion. It can be shown that the solution for the ASEP with reflecting boundaries can be used to described the single file diffusion on a confined interval in the external force field. The crucial difference is that in case of single file diffusion particles are allowed to move continuously instead of lattice hopping in ASEP. Interestingly, a proper generalized Bethe-ansatz can be used to solve for the dynamics in this problem as well [37].

The mapping from polymer to particles is not restricted to the case of pinned polymer loop. Other situations can be investigated with the same mapping, which leads to ASEP model with different boundaries and particle numbers. Moreover, the polymer dynamics beyond 1D is also possible to model by multi-species ASEP model [39, 40]. We believe that by showing the unity of such apparently different systems we pave the way to their better understanding and hopefully to further new results.

ACKNOWLEDGMENTS

We would like to acknowledge stimulating discussions with S. Majumdar and E. Frey.

Appendix A: Stationary statistics

We mention in the main text three different ways to get the stationary statistics. We will compare and bench-

mark the results here.

The first methods is an approximation method use *grand canonical ensemble* and the technique of Brownian bridge. The approach is sketched in the main text, we will show here the stationary statistics of the pinned 1D polymer, i.e., mean and variance of monomers position.

According to Eq. (2) and Eq. (5a), the mean position of the 1D polymer monomer can be written as

$$\langle z_i \rangle = a\left(2\sum_{j=1}^{i}\mathbb{E}\left[Z_j\right] - i\right) \tag{A1}$$

The variance of monomer position is given by Eq. (5b) and Eq. (7). Plug in Eq. (4) and convert the summation to integral when $T \gg 1$, we obtain

$$\langle z_i \rangle = 2a\tilde{T}\ln\left[\frac{1+\exp\left(\frac{L}{2\tilde{T}}\right)}{\exp\left(\frac{i}{2\tilde{T}}\right)+\exp\left(\frac{L-i}{2\tilde{T}}\right)}\right] \tag{A2a}$$

$$\mathrm{var}\left[z_i\right] = 2a^2\tilde{T}\frac{\sinh\left(\frac{L-i}{2\tilde{T}}\right)\sinh\left(\frac{i}{2\tilde{T}}\right)}{\sinh\left(\frac{L}{2\tilde{T}}\right)\cosh^2\left(\frac{L-2i}{4\tilde{T}}\right)} \tag{A2b}$$

where $\tilde{T} = k_BT/2Fa$.

The second method use *canonical ensemble* with number partition theory and the third method use Bethe-ansatz obtaining the stationary state of ASEP are both exact solution. We will show the exact partition function obtained from these two methods are equivalent and then compare the exact result of density profile to the *Fermi-Dirac* approximation of the first method.

The exact term of partition function from method two is already listed in Eq. (10). So let us derive here the exact partition function using method three. According to the rules of our generalised Bethe-ansatz, the N particles stationary solution of the ASEP system can be constructed as

$$P^e(x_1, x_2, \cdots, x_N) = \Psi_0(x_1, x_2, \cdots, x_N) = A\prod_{j=1}^{N}\left(\frac{\alpha}{\beta}\right)^{x_j} \tag{A3}$$

One can plug it in the master equation check that the corresponding eigenvalue $\Lambda_0 = 0$, and also verify the exclusive condition as well as the reflecting boundaries are both fulfilled. Remember that $\alpha/\beta = \exp\left(-\Delta E/k_BT\right)$, one can see clearly the connection between Eq. A3 and the partition function after do a variable transfer and rewrite it as

$$P^e(x_1, x_2, \cdots, x_N) = A\exp\left(-\frac{\Delta E}{k_BT}E\right) \tag{A4}$$

where $E := \sum_j x_j - E_0$ with $E_0 = 1 + 2 + \cdots + N = \frac{N(N+1)}{2}$. So E is a integer in the range of $0, 1, \cdots, N(L-N)$. One immediately recognize the partition function is related to the normalization prefactor A as following:

$$\mathcal{Z}(T) = A^{-1} = \sum_{x_1<x_2<\cdots<x_N} q^{\sum_j x_j} = q^{E_0}\sum_{E=0}^{N(L-N)} g(E)q^E \tag{A5}$$

And $g(E)$ is exact the number of partitions of positive integer E to N parts with each of size at most $L-N$. Further more, we can also identify the Gaussian binomial coefficients

$$\sum_{E=0}^{N(L-N)} g(E)q^E = \binom{L}{N}_q = \frac{[L]_q!}{[L-N]_q![N]_q!} \tag{A6}$$

where $[N]_q = 1+q+q^2+\cdots+q^{N-1}$ is called a q number. So we finally arrive at Eq. (21). Meanwhile, by setting $E_0 = 0$ and $N = L/2$ as we did in section II C, we obtain exactly the same partition function as Eq. (10). We emphasize here that both methods give us correct exact stationary statistics. However, use the Bethe-ansatz method, one can step further into the dynamics.

With the stationary N particle distribution Eq. (21), we can readily calculate the equilibrium distribution of any tagged particle. Denote he distribution of the nth particle $p_n(x)$, we have

$$\begin{aligned} p_n(x) &= \sum_{0<x_1<\cdots<x_{n-1}\le x-1} P^e(x_1, x_2, \cdots, x_N) \\ &\quad\times \sum_{x<x_{n+1}<\cdots<x_N\le L} P^e(x_1, x_2, \cdots, x_N) \\ &= q^{(N+1-n)(x-n)}\binom{x-1}{n-1}_q\binom{L-x}{N-n}_q\Big/\binom{L}{N}_q \end{aligned} \tag{A7}$$

Finally, the equilibrium density profile, which is the exact counterpart of Fermi-Dirac distribution Eq. (4), can be obtain by summing up $p_n(x)$

$$\rho(x) = \sum_{n=1}^{N} p_n(x) \tag{A8}$$

The exact result is shown in Fig. 7 and compared with the density profile we get from the Fermi-Dirac approximation.

Appendix B: Derivation of the Bethe Equations

To show the derivation of the Bethe Equations, we first show it in the simple two particles case and then generalise to N particles case.

We start by writing down the master equation for the two-particle density assuming both of the particles are neither sitting on the boundary sites nor sitting on the

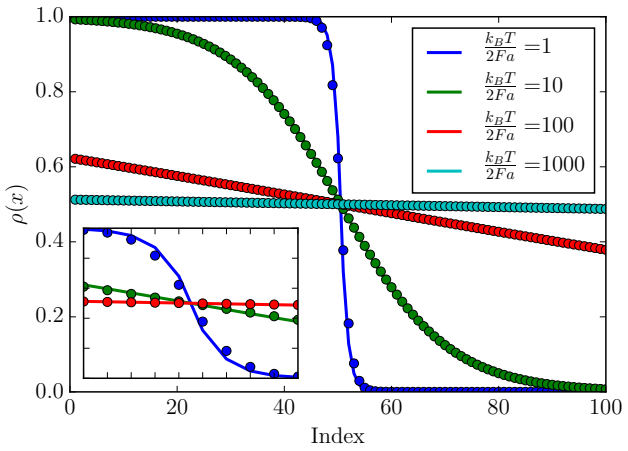

FIG. 7. density profile

neighboring sites:

$$\begin{aligned}\frac{dP(x_1,x_2;t)}{dt} =&\alpha P(x_1-1,x_2;t)+\beta P(x_1+1,x_2;t)\\ &+\alpha P(x_1,x_2-1;t)+\beta P(x_1,x_2+1;t)\\ &-2(\alpha+\beta)P(x_1,x_2;t)\end{aligned} \tag{B1}$$

where $P(x_1,x_2;t)$ is time dependent probability of finding the first and the second particle at coordinates (x_1,x_2) respectively. The master equation B1 should be supplemented with reflecting boundary conditions [41]

$$\alpha P(0,x_2;t)=\beta P(1,x_2;t) \tag{B2a}$$
$$\alpha P(x_1,L;t)=\beta P(x_1,L+1;t) \tag{B2b}$$

and with the exclusion condition (two particles can not occupy the same lattice site)[32]:

$$\alpha\Psi(x,x)+\beta\Psi(x+1,x+1)=(\alpha+\beta)\Psi(x,x+1), \tag{B3}$$

where x is a shorthand notation for $x_1=x_2=x$ and the above equation (B3) must be valid over all lattice sites. Master Eq. (B1) together with boundary conditions Eqs. (B2) and (B3) define the dynamics of the two particles system. Now let us take the ansatz Eq. (16) and consider two different types of non-stationary eigenmode separately.

Let us firstly consider the two particles non-stationary eigenmode that two classes of building functions are both non-stationary. Plug the ansatz Eq. (16) in the reflecting boundaries Eq. (B2), we get

$$\frac{A_{1+}}{A_{1-}}=-\frac{\alpha-\sqrt{\alpha\beta}e^{-ip_1}}{\alpha-\sqrt{\alpha\beta}e^{ip_1}} \tag{B4a}$$
$$\frac{\tilde{A}_{1+}}{\tilde{A}_{1-}}=-\frac{\left(\alpha-\sqrt{\alpha\beta}e^{-ip_1}\right)e^{-ip_1L}}{\left(\alpha-\sqrt{\alpha\beta}e^{ip_1}\right)e^{ip_1L}} \tag{B4b}$$
$$\frac{\tilde{A}_{2+}}{\tilde{A}_{2-}}=-\frac{\alpha-\sqrt{\alpha\beta}e^{-ip_2}}{\alpha-\sqrt{\alpha\beta}e^{ip_2}} \tag{B4c}$$
$$\frac{A_{2+}}{A_{2-}}=-\frac{\left(\alpha-\sqrt{\alpha\beta}e^{-ip_2}\right)e^{-ip_2L}}{\left(\alpha-\sqrt{\alpha\beta}e^{ip_2}\right)e^{ip_2L}} \tag{B4d}$$

On the other hand, plug the ansatz into the exclusive condition Eq. (B3) and use the definition of $a(p,p')$, we obtain

$$\frac{A_{1+}A_{2+}}{\tilde{A}_{1+}\tilde{A}_{2+}}=-\frac{a(p_1,p_2)}{a(p_2,p_1)} \tag{B5a}$$
$$\frac{A_{1+}A_{2-}}{\tilde{A}_{1+}\tilde{A}_{2-}}=-\frac{a(p_1,-p_2)}{a(-p_2,p_1)} \tag{B5b}$$
$$\frac{A_{1-}A_{2+}}{\tilde{A}_{1-}\tilde{A}_{2+}}=-\frac{a(-p_1,p_2)}{a(p_2,-p_1)} \tag{B5c}$$
$$\frac{A_{1-}A_{2-}}{\tilde{A}_{1-}\tilde{A}_{2-}}=-\frac{a(-p_1,-p_2)}{a(-p_2,-p_1)} \tag{B5d}$$

Notice that the ratio of amplitude coefficients calculated use different ways should be consistent, thus we have the following consistency conditions:

$$\frac{A_{1+}}{A_{1-}}\frac{\tilde{A}_{1-}}{\tilde{A}_{1+}}=\frac{A_{1+}A_{2+}}{\tilde{A}_{1+}\tilde{A}_{2+}}\frac{\tilde{A}_{2+}\tilde{A}_{1-}}{A_{2+}A_{1-}} \tag{B6a}$$
$$\frac{\tilde{A}_{2+}}{\tilde{A}_{2-}}\frac{A_{2-}}{A_{2+}}=\frac{\tilde{A}_{1+}\tilde{A}_{2+}}{A_{1+}A_{2+}}\frac{A_{1+}A_{2-}}{\tilde{A}_{1+}\tilde{A}_{2-}} \tag{B6b}$$

After substitute Eq. (B4),(B5) we arrive at the following Bethe equations:

$$e^{i2p_1L}=\frac{a(p_1,p_2)}{a(p_2,p_1)}\frac{a(p_2,-p_1)}{a(-p_1,p_2)} \tag{B7a}$$
$$e^{i2p_2L}=\frac{a(p_2,p_1)}{a(p_1,p_2)}\frac{a(p_1,-p_2)}{a(-p_2,p_1)} \tag{B7b}$$

For the case that the ansatz is constructed by one stationary and one non-stationary building function classes, the procedure is more or less the same, we can obtain the Bethe equation exact leads to the eigenvalues of single particle spectrum, i.e. $e^{i2p_2L}=1$.

Let us now generalise the calculation to the N particles case, the reflecting boundaries give

$$\frac{A^{\sigma|\sigma(1)=n}_{n+}}{A^{\sigma|\sigma(1)=n}_{n-}}=-\frac{\alpha-\sqrt{\alpha\beta}e^{-ip_n}}{\alpha-\sqrt{\alpha\beta}e^{ip_n}} \tag{B8a}$$
$$\frac{A^{\sigma|\sigma(N)=n}_{n+}}{A^{\sigma|\sigma(N)=n}_{n-}}=-\frac{\left(\alpha-\sqrt{\alpha\beta}e^{-ip_n}\right)e^{-ip_nL}}{\left(\alpha-\sqrt{\alpha\beta}e^{ip_n}\right)e^{ip_nL}} \tag{B8b}$$

and the exclusive conditions implies

$$\frac{A^{\sigma}_{n\pm}A^{\sigma}_{(n+1)\pm}}{A^{\sigma|n\leftrightarrow n+1}_{n\pm}A^{\sigma|n\leftrightarrow n+1}_{(n+1)\pm}}=-\frac{a(\pm p_n,\pm p_{n+1})}{a(\pm p_{n+1},\pm p_n)} \tag{B9}$$

Finally, use the consistency conditions similar to Eq. (B6) we obtain

$$e^{i2p_nL}=\prod_{m\neq n}^{N}\frac{a(p_n,p_m)}{a(p_m,p_n)}\frac{a(p_m,-p_n)}{a(-p_n,p_m)} \tag{B10}$$

Now it would be interesting to interpret the Bethe Equation and compare with the well know Bethe Equation of periodic boundary case. We can consider Eq.

(B8) as a reflector that reflects the particle and change the direction of wave vector, i.e., $p_n \leftrightarrow -p_n$. On the other hand, Eq. (B9) can be interpreted as a permutator that permutes two neighboring particles $n \leftrightarrow (n+1)$. Let us say particle 1 starts from the left side of the lattice and then permutes with all the particle at right side until reaches the right boundary (of course in case of two particles, there are only one particle at the right side), and then reflects by the boundary, become a particle traveling in the opposite direction, and then permutes with all the left side particles until reaches the left side boundary, and then reflects again, which recovers the initial state. In this sense, the particle works as if it is on a lattice with periodic boundary. Use this interpretation and the well know result of periodic Bethe Equation, once can easily recover exactly Eq. (22).

Appendix C: Simulation Methods

Extensive simulations are performed in this work in order to compare with the theory, including the Monte-Carlo simulation of the ASEP system and Brownian Dynamics simulation of the 3D pinned polymer loop. For the ASEP system, Gillespie algorithm [20] is employed for the simulations and we will not go into the details. Interested readers can see the references therein. On the other hand, the Brownian Dynamics simulation is more tricky and we will discuss in the following text.

As we use the simple freely jointed bead-rod model, the Brownian dynamics of the beads ignoring inertial can be written as

$$\xi \frac{d\mathbf{r}_i}{dt} = \mathbf{F}_i^c + \mathbf{F}_i^e + \mathbf{F}_i^b + \mathbf{F}_i^{pseudo} \tag{C1}$$

where ξ is the friction coefficient, $\mathbf{F}_i^c$ is the constraint force that keeps the rod with constant length, $\mathbf{F}_i^e$ is the external force, $\mathbf{F}_i^b$ is the Brownian force that satisfying $\left\langle \mathbf{F}_i^b \right\rangle = \mathbf{0}$ and $\left\langle f_{im}^b(t) f_{jn}^b(t') \right\rangle = 2\xi k_B T \delta_{ij} \delta_{mn} \delta(t - t')$, and $\mathbf{F}_i^{pseudo}$ is pseudo force added in order to get correct statistics, where $\mathbf{F}_i^{pseudo} = -\frac{\partial U_{met}}{\partial \mathbf{r}_i}; U_{met} = \frac{1}{2} k_B T \ln(\det G)$, G is the metric tensor [42].

The constraint force $\mathbf{F}_i^c$ is solved implicitly use the predictor-corrector algorithm by solving the constraint equations that $|\mathbf{r}_{i+1} - \mathbf{r}_i| = a$. On the other hand, in order to pin the polymer loop, we add a "phantom" rod of length zero at the pinned bead, and bond it to the origin.

In practice, we use the dimensionless term of the dynamical equations that can be obtained by the rescaling $\mathbf{r}' \to \mathbf{r}/a$; $t' \to t/(\xi a^2/k_B T)$; $\mathbf{F}' \to \mathbf{F}/(k_B T/a)$.

[1] D. Wirtz, Phys. Rev. Lett. **75**, 2436 (1995).
[2] S. R. Quake, H. Babcock, and S. Chu, Nature **388**, 151 (1997).
[3] Y. T. Lin, D. Frömberg, W. Huang, P. Delivani, M. Chacón, I. M. Tolić, F. Jülicher, and V. Zaburdaev, Phys. Rev. Lett. **115**, 208102 (2015).
[4] S. Jun and A. Wright, Nat. Rev. Microbiol. **8**, 600 (2010), arXiv:NIHMS150003.
[5] J. D. Halverson, J. Smrek, K. Kremer, and A. Y. Grosberg, Reports Prog. Phys. **77**, 022601 (2014), arXiv:arXiv:1311.5262v1.
[6] L. Giorgetti, R. Galupa, E. P. Nora, T. Piolot, F. Lam, J. Dekker, G. Tiana, and E. Heard, Cell **157**, 950 (2014).
[7] R. K. Sachs, G. van den Engh, B. Trask, H. Yokota, and J. E. Hearst, Proc. Natl. Acad. Sci. **92**, 2710 (1995).
[8] B.-Y. Ha and Y. Jung, Soft Matter **11**, 2333 (2015).
[9] T. Mizuguchi, J. Barrowman, and S. I. Grewal, FEBS Lett. **589**, 2975 (2015).
[10] P.-G. G. de Gennes, *Scaling Concepts in Polymer Physics* (Cornell University Press, 1979).
[11] M. Doi and S. F. Edwards, *The theory of polymer dynamics* (Oxford University Press, 1988).
[12] David Chandler, *Introduction to modern statistical mechanics.*, Vol. 1 (Oxford University Press, 1987).
[13] K. Huang, *Statistical Mechanics*, 2nd ed. (John Wiley & Sons, 1987) p. 493.
[14] B. Derrida, Phys. Rep. **301**, 65 (1998).
[15] P. C. Bressloff, J. M. Newby, and B. Derrida, Rev. Mod. Phys. **301**, 135 (2013).
[16] G. Schütz, in *Phase Transitions Crit. Phenom.*, Vol. 19 (Academic Press, 2001) pp. 1–251.
[17] J. de Gier and F. H. L. Essler, Phys. Rev. Lett. **95**, 240601 (2005).
[18] D. Simon, J. Stat. Mech. Theory Exp. **2009**, P07017 (2009), arXiv:0903.4968.
[19] M. T. Batchelor, Phys. Today **60**, 36 (2007).
[20] D. T. Gillespie, J. Comput. Phys. **22**, 403 (1976).
[21] C. Cruz, F. Chinesta, and G. Régnier, Arch. Comput. Methods Eng. **19**, 227 (2012).
[22] M. Somasi, B. Khomami, N. J. Woo, J. S. Hur, and E. S. Shaqfeh, J. Nonnewton. Fluid Mech. **108**, 227 (2002).
[23] D.-Q. Ding, A. Yamamoto, T. Haraguchi, and Y. Hiraoka, Dev. Cell **6**, 329 (2004).
[24] S. K. Vogel, N. Pavin, N. Maghelli, F. Jülicher, and I. M. Tolić-Nørrelykke, PLoS Biol. **7**, e1000087 (2009).
[25] R. Koszul and N. Kleckner, Trends Cell Biol. **19**, 716 (2009), arXiv:NIHMS150003.
[26] G. F. Lawler and V. Limic, *Random Walk: A Modern Introduction* (Cambridge University Press, Cambridge, 2010).
[27] I. Kovalenko, USSR Comput. Math. Math. Phys. **8**, 353 (1968).
[28] K. B. Athreya and S. N. Lahiri, *Measure Theory and Probability Theory* (Springer, 2006).
[29] L. M. Sander, *Advanced Condensed Matter Physics* (Cambridge University Press, 2009).
[30] G. E. Andrews, *The Theory of Partitions*, Cambridge mathematical library (Cambridge University Press, 1998).
[31] S. Sandow and G. Schütz, Europhys. Lett. **26**, 7 (1994).
[32] K. Mallick, J. Stat. Mech. Theory Exp. **2011**, P01024 (2011), arXiv:arXiv:1101.2849v1.

[33] E. Brattain, N. Do, and A. Saenz, , 1 (2015), arXiv:1511.03762.
[34] P. Pincus, Macromolecules **9**, 386 (1976).
[35] F. Brochard-Wyart, Europhys. Lett. **30**, 387 (1995).
[36] T. Perkins, Quake, D. Smith, and S. Chu, Science (80-.). **264**, 822 (1994).
[37] L. Lizana and T. Ambjörnsson, Phys. Rev. Lett. **100**, 200601 (2008).
[38] E. Barkai and R. Silbey, Phys. Rev. Lett. **102**, 050602 (2009).
[39] O. Golinelli and K. Mallick, J. Phys. A. Math. Gen. **39**, 12679 (2006), arXiv:0611701 [cond-mat].
[40] A. Lazarescu, J. Phys. A Math. Theor. **48**, 503001 (2015), arXiv:1507.04179.
[41] N. G. van. Kampen, *Stochastic processes in physics and chemistry* (Elsevier, 2007) p. 463.
[42] M. Pasquali and D. C. Morse, J. Chem. Phys. **116**, 1834 (2002).